Optical Engineering

SPIEDigitalLibrary.org/oe

Broadband and low-power bright soliton propagation in line-defect photonic crystal waveguide

Huiping Tian
Daquan Yang
Lingyu Liu
Yuefeng Ji

SPIE

Broadband and low-power bright soliton propagation in line-defect photonic crystal waveguide

Huiping Tian
Daquan Yang
Lingyu Liu
Yuefeng Ji
Beijing University of Posts and Telecommunications
State Key Laboratory of Information Photonics and Optical Communications
School of Information and Communication Engineering
Beijing 100876, China
E-mail:hptian@bupt.edu.cn

Abstract. The broadband and low-power optical bright soliton propagation in a line-defect photonic crystal waveguide (PCW) is obtained. The line-defect PCW is composed by polystyrene background material and Si-rods. By adjusting the PCW structure parameters, optical bright soliton in the optimized PCW structures with a bandwidth of 2.35 nm/3.61 nm and a peak power as low as 8.1 μW/35.7 μW is achieved. For a dense wavelength division multiplexing system with 0.2 nm of channel spacing in optical fiber communications, 8 and 16 channels can be supported within the 2.35-nm and 3.61-nm bandwidths. The peak power range is within the power range of the optical fiber communication criterion. [DOI: 10.1117/1.OE.52.5.055006]

Subject terms: optical soliton; bandwidth; peak power; photonic crystal waveguide.

Paper 130103 received Jan. 22, 2013; revised manuscript received Apr. 8, 2013; accepted for publication Apr. 25, 2013; published online May 22, 2013.

1 Introduction

In recent years, integrated optical technology has been a research focus in optical communication networks.[1] However, compared with electronics, the integration scale and integration level of optical devices are still fairly low.[2,3] As an advanced technique, the photonic crystal waveguide (PCW) may eventually provide a way to achieve on-chip photonic integration with room-temperature operation. PCW has many advantages, such as a high degree of control, great potential bandwidth, and fine optical operation properties such as realizing slow light property.[4,5] To date, slow light based on PCW has been a hot topic due to its broad range of applications, including optical delay lines and data synchronization in optical communications and information processing systems.[6–8] Meanwhile, as an important nonlinear phenomenon and shape-unchanged optical pulse, optical soliton in photonic crystal fiber and PCW has been researched extensively. For example, Lefrançois et al.[9] researched the scaling of dissipative soliton fiber lasers to megawatt peak powers by use of large-area photonic crystal fiber. Stark et al.[10] studied soliton blue shift in tapered photonic crystal fibers, and Colman et al.[11] researched temporal solitons and pulse compression in PCW. Using soliton pulses as information carriers in PCW not only can obtain pulse propagation without waveform distortion, but also can realize slow light property.[12–14] This has opened a new avenue toward exploiting the low group velocity that PCW has exhibited.

However, the previous studies of soliton propagation in PCWs[12–14] have focused only on soliton propagation in the conventional PCW, and the bandwidth of soliton propagation at the given group index is extremely narrow.[12–15] This is because the group index near the band edges has a large change, so the bandwidth at the given group index is quite narrow. To the best of our knowledge, the bandwidth improvement of soliton propagation in PCW has not been analyzed. For practical applications, it is quite necessary to extend the bandwidth for the soliton propagation at a given group index. Moreover, the required peak power must be optimized to adapt to the application criterion, since the peak power obtained in previous works on soliton propagation in PCW[12–14] is a little large. Our research work indicates that the bandwidth and peak power can be further improved by optimizing the PCW structure parameters.

In this paper, we focus on the bandwidth improvement and peak power reduction of the bright soliton propagation in line-defect PCW. First, we propose a method to improve the bandwidth of bright soliton propagation near the right band edge of the guided mode in PCW. Second, we focus on optimizing the bandwidth and required peak power by appropriately adjusting the PCW parameters, and the optimized PCW structures are introduced. Finally, the soliton propagation performances of the optimized PCW structures are numerically analyzed.

2 Theoretical Model

2.1 *PCW Model*

The basic PCW model in this paper consists of a single line defect and triangular lattice rods as shown in Fig. 1. The lattice constant is a. The radius of the first two rows of rods adjacent to the defect is denoted by r_1, the radius of the second two rows is r_2, and the radius of the remaining rows is $r = 0.215a$. The figures Δx_1 and Δx_2 represent the shift of the first and second two rows adjacent to the defect along waveguide axis, respectively. Dy is the conventional distance between the two adjacent rows, which becomes dy by changing the distance between the two adjacent rows. The refractive indexes of the background material polystyrene and the Si-rods are 1.59 and 3.5, respectively. The nonlinear refractive indexes[12,16] of Si and polystyrene are $n_{2-\mathrm{Si}} = 1.5\times 10^{-16}$ m^2/W and $n_{2-\mathrm{polystyrene}} = -9.3\times 10^{-13}$ m^2/W. Based on this model, by adjusting the structure parameters, we can optimize the bandwidth and peak power of soliton propagation and get broadband and low power bright soliton propagation. The soliton propagation mode is discussed below.

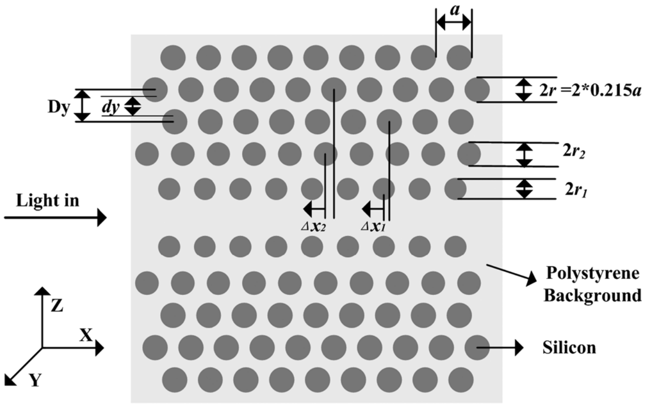

Fig. 1 Schematic of the line-defect PCW with Si-rods and polystyrene background.

2.2 *Model of the Nonlinear Pulse Propagation in PCW*

The nonlinear propagation model of optical pulses inside a PCW satisfies the equation[12,17]

$$j\left(\frac{\delta A}{\delta z}+\frac{\Gamma}{2A}\right)+\sum_{i\geq 2} j^{m(l)}\frac{\beta_l \delta^l A}{l!\delta T^l}+\gamma|A|^2 \qquad A=0, \tag{1}$$

where A is the temporal envelope of the electric field along the PCW, the coefficient Γ is related to the optical losses, z is the propagation distance, the function $\mathrm{m}(l)$ is defined as $\mathrm{m}(l)=\mathrm{mod}(l,2)$, β_l is the group velocity dispersion (GVD) coefficient (for $l=2$) or a higher-order dispersion coefficient (for $l>2$), and γ is the self-phase modulation (SPM) coefficient.

From Eq. (1), the well-known nonlinear Schroedinger equation, we know that, if $\beta_2<0$, bright soliton can be supported. In common PCW, near the left band edge, β_2 can be negative and support bright solitons.[12] The initial condition for the bright soliton solution can be given[12,17] as

$$A(0,T)=\sqrt{P_0}\ \sec\ h(T/T_0), \tag{2}$$

where T_0 is the initial soliton width determined by $T_0\approx t_{\mathrm{FWHM}}/1.76$, t_{FWHM} is the full width at half maximum (FWHM) of the pulse, and P_0 is the required soliton peak power, determined[12,17] by

$$P_0\cong N^2 49.5\frac{|\beta_2|}{\gamma}{R_b}^2, \tag{3}$$

where R_b is the bit rate of the optical signal, and N is the soliton order. For the fundamental soliton, $N=1$. For β_2, it is well known that

$$\beta_2=\frac{\mathrm{d}(v_g^{-1})}{\mathrm{d}\omega}=\frac{1}{c}\times\frac{\mathrm{d}n_g}{\mathrm{d}\omega}=\frac{\mathrm{d}^2 k}{\mathrm{d}\omega^2}, \tag{4}$$

where ω is the normalized frequency, k is the wave vector, c is the light velocity in vacuum, and v_g is the group velocity, which can be obtained by the slope of the dispersion curve of guide mode as

$$v_g=\frac{\partial\omega}{\partial k}=\frac{c}{n_g}, \tag{5}$$

where $n_g=n+\omega(\mathrm{d}n/\mathrm{d}\omega)$ is the group index. The dispersion curve of the guide mode is determined by the PCW parameters and can be obtained by plane wave expansion (PWE). Then β_2 and v_g can be calculated by deriving the dispersion curve. For γ, it can be calculated by the optical field distribution and the PCW parameters. The optical field distribution can be obtained by the finite-difference time-domain technique (FDTD) and by PCW parameters. In this paper, we will determine the bandwidth and peak power optimization near the right band edge for soliton propagation by adjusting the parameters of the above PCW and by following the above theory model.

3 Simulation Results

3.1 *Bandwidth Improvement of Soliton Propagation in PCW*

The group index and GVD curves for TM polarized mode in PCW are numerically calculated by the 2D PWE method. The defect mode inside the band gap is studied with a super cell that is 1 unit in the x-direction and 10 units in the z-direction in the PWE calculation.

Figure 2 shows the group index and group velocity dispersion of the initial PCW structure (shown in Fig. 1) without any structure parameter adjusted. The minimum and maximum values of K represent the left and right band edges of the guided mode, respectively.[12] The GVD curve in the inset figure indicates that the dispersion relation is $\beta_2<0$ near the left band edge, so the bright soliton can be considered in this case.[12] The bright soliton propagation near the left band edge of the guided mode in PCW has been studied previously,[12–15] but the bandwidth for bright soliton propagation was extremely narrow. Moreover, near the right band edge of the mode, $\beta_2>0$, the bright soliton cannot be supported, which is the same situation as in Thomas's work.[12–14]

Here, the bandwidth improvement of slow light based on the soliton propagation is obtained by adjusting PCW structure parameters Δx_1 and Δx_2. In our work, better bandwidth performance is obtained when $\Delta x_1=0.2a$, $\Delta x_2=0.344a$, and the PCW structure is defined as PCW-I. Figure 3 shows the group index n_g and GVD β_2 of PCW-I. The inset picture indicates n_g and β_2 near the right band edge. By adjusting Δx_1 and Δx_2, near the right band edge of

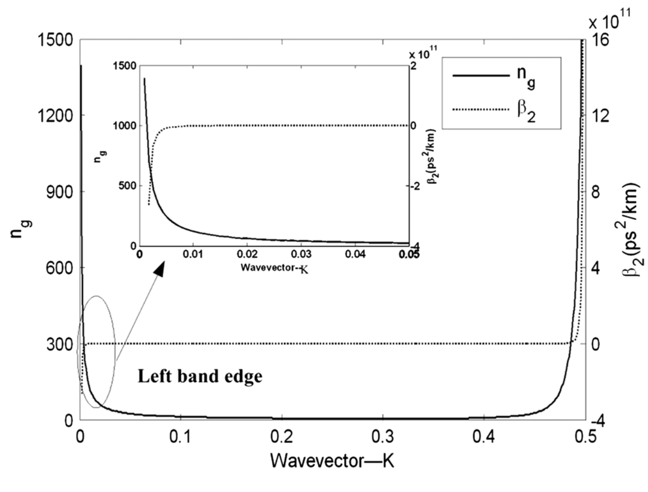

Fig. 2 Group index and group velocity dispersion of the initial PCW structure.

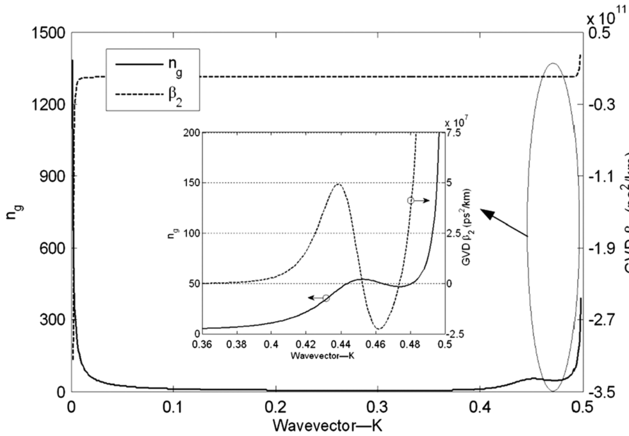

Fig. 3 Group index and group velocity dispersion of PCW-I.

the guided mode, a region appears where the group index n_g can be considered as constant[3] with a range of $\pm 10\%$. In addition, as shown in the figure, within the region of constant n_g, part of the GVD is $\beta_2 < 0$, so the bright soliton can be considered. This is distinguished from the results of previous PCW structure research[12–15] in that, near the right band edge, $\beta_2 > 0$, and bright soliton cannot be considered in the initial PCW structure.

In this paper, for bright soliton propagation, the bandwidth is defined as the frequency (wavelength) range where $\beta_2 < 0$. Figure 4 shows the relationships between the GVD coefficient β_2 and the wavelength for the bandwidth range of $\beta_2 < 0$ for PCW-I. The solid-dotted curve is β_2 versus the wavelength. In this PCW, the bandwidth for $\beta_2 < 0$ is 1.96 nm, which is defined as BW-All. Therefore, the bright soliton of Eq. (2) can be supported in BW-All. According to Eq. (3), it can be easily deduced that the required soliton peak power P_0 is different at different values of β_2, so it is different at different wavelengths. In practical applications, it is hard to have precise control of the peak power P_0 for soliton propagation. This problem can be solved by using perturbation methods developed for soliton stability research. When the peak power does not exactly match the value of $N = 1$, mathematically, if $0.5 \le N \le 1.5$, solitons can be formed, though the peak power P_0 varies within a large range.[17] The two dashed lines in Fig. 4 show the maximum and minimum of β_2 and the peak power.

For PCW-I, as shown in Fig. 4, within BW-All, the maximum GVD is $\beta_{\max} = -2.24 \times 10^7\ \mathrm{ps^2/km}$ (the lower

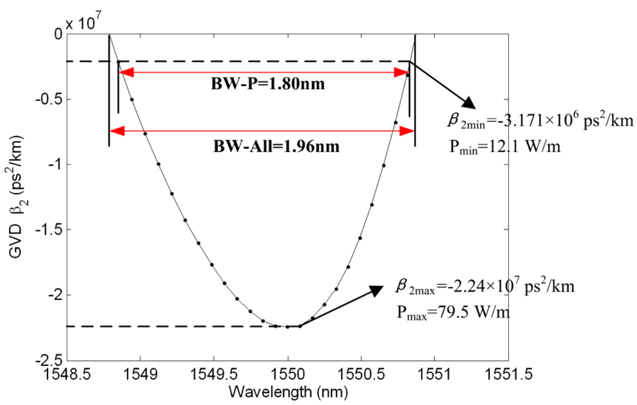

Fig. 4 Two kinds of bandwidth (B-All and B-Power) for PCW-I.

dashed line), and the calculated required soliton peak power is $P_{\max} = 79.5\ \mathrm{W/m}$. To get a bandwidth in a continuous wavelength range, $P_{\max} = 79.5\ \mathrm{W/m}$ corresponds to $N = 1.5$. Then, according to Eq. (3), the minimum peak power is $P_{\min} = 12.1\ \mathrm{W/m}$, which corresponds to $N = 0.5$, and the corresponding GVD is $\beta_{\min} = -3.171 \times 10^6\ \mathrm{ps^2/km}$ (the higher dashed line). If the input soliton peak power is $P_0 = 35.4\ \mathrm{W/m}$, which is calculated by $P_0 = 0.5 \times P_{\max} = 1.5 \times P_{\min}$, this satisfies the condition that $0.5 \le N \le 1.5$. Hence, the soliton can form and propagate at the constant input peak power of $P_0 = 35.4\ \mathrm{W/m}$ within the bandwidth, and the bandwidth for this is about 1.8 nm, which is defined as BW-P.

So far, BW-All and BW-P have been defined, and their calculations have been given. Within BW-All, the required soliton peak power P_0 is different at different wavelengths, but within BW-P, only one peak power P_0 is needed. As to PCW-I, BW-All is 1.96 nm, and BW-P is 1.8 nm. The required power P can be estimated by multiplying the power density P_0 by ω_{eff}. After calculating the field in the supercell, the effective mode aperture of PCWs in this paper is about $\omega_{\mathrm{eff}} = 0.5\ \mu\mathrm{m}$, which is the same as that in Theocharidis et al.[12] Here, it can be calculated that bright soliton can propagate during BW-P only for one peak power of $P = P_0 \times \omega_{\mathrm{eff}} = 35.4\ \mathrm{W/m} \times 0.5\ \mu\mathrm{m} = 17.7\ \mu\mathrm{W}$. Meanwhile, n_g approaches a constant of about 51.

3.2 *Optimizing of Bandwidth and Peak Power*

In this section, the bandwidth and required soliton peak power are optimized by adjusting the PCW structure parameters r_1, r_2, and dy step by step. The group index and group velocity dispersion of the two final optimized PCW structures, which are defined as PCW-II and PCW-III, are shown in Fig. 5(a) and 5(b). The PCW parameters are given in Table 1. Figure 5(a) indicates that, after being optimized, a much larger flat band appears around the work wavelength of 1,550 μm in the group velocity curve for the two cases. This means that, physically, the bandwidth is improved. Figure 5(b) clearly shows that, among the flat band ranges, a region exists where $\beta_2 < 0$ for the two cases. In physics, the bright soliton can be supported. The concreted performance parameters such as bandwidth and power are also shown in Table 1. This table gives a summary and comparison of the structure parameters and soliton performance (when $R_b = 100\ \mathrm{Gb/s}$) of the two optimized PCWs we have found. Detailed descriptions are given below.

PCW-II is obtained by adjusting r_1 and r_2 for PCW-I. As shown in Table 1 and in the dotted lines of Fig. 5(a) and 5(b), compared with PCW-I, PCW-II has an improved bandwidth, BW-All increases from 1.96 nm to 2.47 nm, and BW-P increases from 1.8 nm to 2.35 nm. Also, n_g has decreased from 51 to 38. At the same time, it can be found that the peak power P is only about 8.1 μW when n_g is 38 — a 7.53×10^7 times reduction[9] compared with $P = 6.1 \times 10^2$ W when $n_g = 30$. Considering the DWDM system with 0.2 nm of channel spacing in optical networks, about 11 channels can be supported within the 2.35-nm BW-P wavelength range.

PCW-III is obtained by adjusting dy in PCW-II. As Table 1 and the solid lines of Fig. 5(a) and 5(b) show, compared with PCW-II, BW-All increases to 4.08 nm (a 1.61-nm improvement), and BW-P increases to 3.61 nm (a 1.26-nm improvement). It can be seen that the bandwidth can be

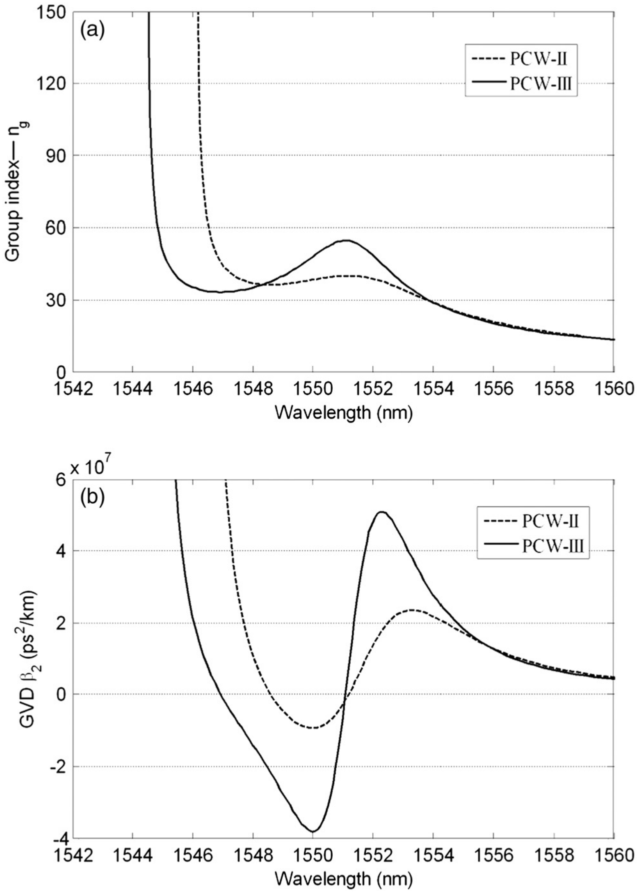

Fig. 5 (a) Group index and (b) GVD of PCW-II and PCW-III.

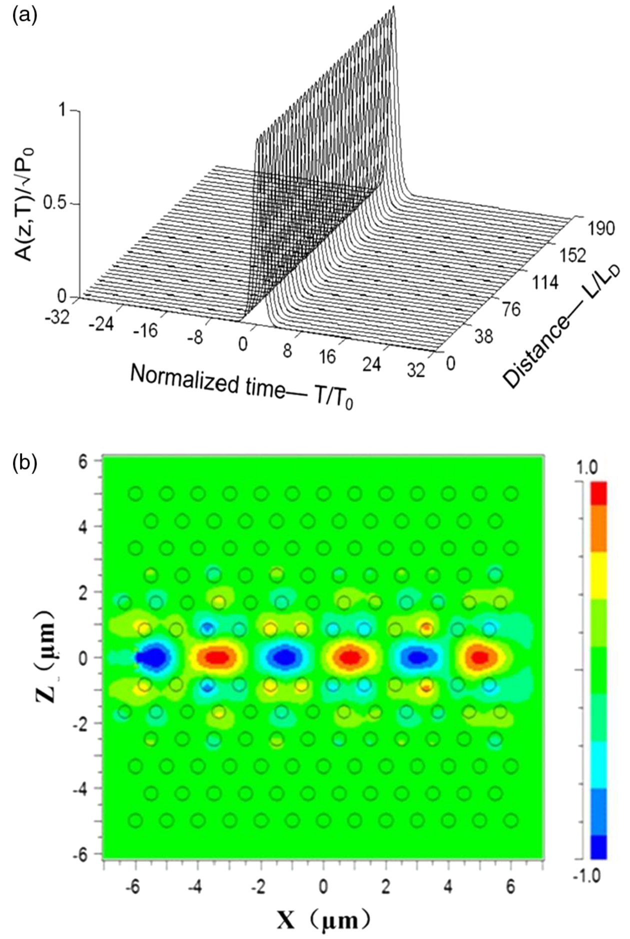

Fig. 6 (a) Bright soliton propagation in PCW-III and (b) field pattern of the designed PCW-III.

further improved, and it can be deduced that dy has a larger impact on the bandwidth improvement than r_1 and r_2. Therefore, about 18 channels can be supported within the 3.61-nm BW-P wavelength range for DWDM application with 0.2 nm of channel spacing. In PCW-III, the soliton peak power P is about 35.7 μW when n_g is 44, of a 1.71×10^7 times reduction[12] from $P = 6.1 \times 10^2$ W when $n_g = 30$.

To summarize, for the two final optimized structures PCW-II and PCW-III, PCW-II has a peak power P as low as 8.1 μW. However, PCW-III has a larger bandwidth, where BW-All is 4.08 nm and BW-P is 3.61 nm. For a DWDM system with 0.2 nm of channel spacing in optical networks, about 11 and 18 channels can be supported in the 2.35- and 3.61-nm bandwidths of PCW-II and PCW-III, respectively. Therefore, DWDM applications with 8 and 16 channels can be realized in PCW-II and PCW-III, respectively. These results indicate that the bandwidth and required peak power for soliton propagation in PCW have been significantly improved in our proposed structures, and the delay based on soliton propagation in PCW can be applied in all-optical networks.

The bright soliton propagation and the field pattern of PCW-III are numerically investigated to verify the above results. Figure 6(a) shows the temporal domain bright soliton propagation in PCW-III with $\beta_{\max} = -3.82 \times 10^7$ ps^2/km and $\gamma = 117.7$ W^{-1}, which is obtained by employing the numerical split-step Fourier method to solve Eq. (1). The curves along the normalized time axis and the amplitude axis in Fig. 6(a) denote the shape of the bright soliton. The initial soliton shape is given from Eq. (2), which is a

Table 1 Structure parameters and soliton performance of the PCWs.

	Structure parameters							Performance	
Structure	a (nm)	r (a)	r_1 (r)	r_2 (r)	dy (D)	Δx_1 (a)	Δx_2 (a)	P (μW)	n_g
PCW-I	482	0.215	1	1	0	0.2	0.344	17.7	51
PCW-II	483	0.215	0.97	0.95	0	0.2	0.344	8.1	38
PCW-III	487	0.215	0.97	0.95	0.96	0.2	0.344	35.7	44

hyperbolic secant function of time. The distance axis L in Fig. 6(a) is in units of the dispersion length L_D. The PCW length is $L = 1$ cm, so the distance is $L = 190 \times L_D$. As shown in Fig. 6(a), the soliton pulse propagates in a stable manner in the PCW along the distance axis without waveform distortion. This means physically that the dispersion and the nonlinearity are balanced. Figure 6(b) shows the spacial field pattern of the optical wave in PCW-III, where the x-axis denotes the longitudinal dimension of PCW-III that corresponds with the distance axis of Fig. 6(a). The z-axis shows the transverse dimension of PCW-III. From Fig. 6(b), it can be seen that the light signal is well confined spatially in PCW-III, and the spatial diffusion and scattering are small. At last, we can combine Fig. 6(a) and 6(b) to determine that the optical wave signal can propagate effectively in PCW-III without temporal dispersion and spatial scattering. As a result, it is especially appealing for optical communication.

4 Conclusion

In this paper, we studied the improvement of bandwidth and power performance for bright soliton propagation near the right band edge in line-defect PCW. The simulation results show that bandwidth improvement of bright soliton propagation can be obtained by properly adjusting the structure parameters Δx_1, Δx_2, r_1, r_2, and dy. In the proposed structure PCW-II, a 2.47-nm BW-All bandwidth for bright soliton propagation with different peak powers is obtained. A 2.35-nm BW-P bandwidth is also obtained, within which a constant peak power as low as 8.1 μW is needed with a constant group velocity about 38. For the proposed structure PCW-III, BW-All is 4.08 nm, and BW-P is 3.61 nm; both figures are larger than those of PCW-II. The constant peak power is 35.7 μW within the 3.61-nm BW-P bandwidth, with a constant group velocity about 44. For a DWDM system with 0.2 nm of channel spacing in optical networks, 8 and 16 channels can be supported within the 2.35-nm and 3.61-nm BW-P bandwidths of PCW-II and PCW-III, respectively. The soliton pulse envelope propagation and the field pattern of the optical wave in the optimized PCW have also been numerically investigated. Our research shows the optimal optical wave propagation performance of the PCW, which can be applied in all-optical network.

Acknowledgments

This research was supported in part by National 973 Program (No. 2012CB315705), National 863 Program (No. 2011AA010303), China.

References

1. T. F. Krauss, "Slow light in photonic crystal waveguides," *J. Phys. D: Appl. Phys.* **40**(9), 2666–2670 (2007).
2. T. Baba, "Slow light in photonic crystals," *Nat. Photon.* **2**(8), 465–473 (2008).
3. F. Long, H. P. Tian, and Y. F. Ji, "A study of dynamic modulation and buffer capability in low dispersion photonic crystal waveguides," *J. Lightwave Technol.* **28**(8), 1139–1143 (2010).
4. D. J. Gauthier, A. L. Gaeta, and R. W. Boyd, "Slow light: from basics to future prospects," *Photon. Spectra* **40**(3), 44–50 (2006).
5. T. Baba and D. Mori, "Potential of slow light in photonic crystal," *Proc. SPIE* **6351**, 63511Z (2006).
6. M. Notomi et al., "Extremely large group velocity dispersion of line-defect waveguides in photonic crystal slabs," *Phys. Rev. Lett.* **87**(25), 253902 (2001).
7. X. Zhang, H. P. Tian, and Y. F. Ji, "Group index and dispersion properties of photonic crystal waveguides with circular and square air-holes," *Opt. Commun.* **283**(9), 1768–1772 (2010).
8. Y. Hamachi, K. Shousaku, and B. Toshihiko, "Slow light with low dispersion and nonlinear enhancement in a lattice-shifted photonic crystal waveguide," *Opt. Lett.* **34**(7), 1072–1074 (2009).
9. S. Lefrançois et al., "Scaling of dissipative soliton fiber lasers to megawatt peak powers by use of large-area photonic crystal fiber," *Opt. Lett.* **35**(10), 1569–1571 (2010).
10. S. P. Stark, A. Podlipensky, and P. St. J. Russell, "Soliton Blueshift in Tapered Photonic Crystal Fibers," *Phys. Rev. Lett.* **106**(8), 083903 (2011).
11. P. Colman et al., "Temporal solitons and pulse compression in photonic crystal waveguides," *Nat. Photon.* **4**(12), 862–868 (2010).
12. A. Theocharidis et al., "Linear and nonlinear optical pulse propagation in photonic crystal waveguides near the band edge," *IEEE. J. Quantum Electron.* **44**(11), 1020–1027 (2008).
13. T. Kamalakis and T. Sphicopoulos, "A new formulation of coupled propagation equations in periodic nanophotonic waveguides for the treatment of kerr-induces nonlinearities," *IEEE. J. Quantum Electron.* **43**(10), 923–933 (2007).
14. I. Neokosmidis, T. Kamalakis, and T. Sphicopoulos, "Optical delay lines based on soliton propagation in photonic crystal coupled resonator optical Waveguides," *IEEE. J. Quantum Electron.* **43**(7), 560–567 (2007).
15. L. Y. Liu, H. P. Tian, and Y. F. Ji, "Soliton pulse propagation and optical delay properties in photonic crystal waveguide," *Acta Phys. Sin.* **60**(10), 104216 (2011).
16. C. R. Mendon et al., "Nonlinear refractive indices of polystyrene films doped with azobenzene dye Disperse Red 1," *Elect. Lett.* **34**(1), 116–117 (1998).
17. G. P. Agrawal, *Nonlinear Fiber Optics*, Academic Press, San Diego (1989).

Huiping Tian received BS and PhD degrees from Shanxi University, China, in 1998 and 2003, respectively. She is an associate professor in the School of Information and Communication Engineering, Beijing University of Posts and Telecommunications (BUPT), China. Her research interests are focused on ultra-short and ultrafast processes in the transmission of optics, photonic crystals, and broadband information networking.

Daquan Yang received a bachelor's degree in electronic information science and technology from JiNan University, China, in 2009. He currently is a master's candidate in the State Key Laboratory of Information Photonics and Optical Communications, Beijing University of Posts and Telecommunications (BUPT), China. His research focuses on photonic crystals and optical communication.

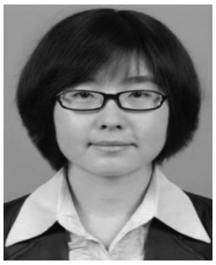

Lingyu Liu received a master's degree in information and communication systems from the State Key Laboratory of Information and Optical Communications, Beijing University of Posts and Telecommunications (BUPT), China, in 2012. Her research focused on nonlinear effects in photonic crystals. She currently works in Jilin province and majors in electric power communication technique.

Yuefeng Ji received a PhD degree from Beijing University of Posts and Telecommunications (BUPT), China, where he is now a professor and executive dean of the Institute of Information Photonics and Optical Communications. His research interests are primarily broadband communication networks and optical communications, with emphasis on key theory, realization of technology, and applications.